

# Ligand-Induced Dynamical Regulation of NO Conversion in *Mycobacterium tuberculosis* Truncated Hemoglobin-N

Axel Bidon-Chanal,<sup>1</sup> Marcelo A. Martí,<sup>2</sup> Alejandro Crespo,<sup>2</sup> Mario Milani,<sup>3</sup> Modesto Orozco,<sup>4</sup> Martino Bolognesi,<sup>3</sup> F. Javier Luque,<sup>1\*</sup> and Darío A. Estrin<sup>2\*</sup>

<sup>1</sup>Departament de Fisicoquímica, Facultat de Farmàcia, Universitat de Barcelona, Av. Diagonal 643, 08028, Barcelona, Spain

<sup>2</sup>Departamento de Química Inorgánica, Analítica y Química Física/INQUIMAE-CONICET, Facultad de Ciencias Exactas y Naturales, Universidad de Buenos Aires, Ciudad Universitaria, Pabellón 2, Buenos Aires, C1428EHA, Argentina

<sup>3</sup>Department of Biomolecular Sciences and Biotechnology, and CNR-INFM, University of Milano, Milano, Italy

<sup>4</sup>Departament de Bioquímica i Biologia Molecular, Facultat de Química, Universitat de Barcelona, Martí i Franquès 1, 08028 Barcelona, Spain; Unidad de Modelización Molecular y Bioinformática, Parc Científic de Barcelona, Josep Samitier 1-6, 08028 Barcelona; Span and Computational Biology Program. Barcelona Supercomputing Center, Edificio Nexus II, Barcelona 08028, Spain

**ABSTRACT** *Mycobacterium tuberculosis*, the causative agent of human tuberculosis, is forced into latency by nitric oxide produced by macrophages during infection. In response to nitrosative stress *M. tuberculosis* has evolved a defense mechanism that relies on the oxygenated form of “truncated hemoglobin” N (trHbN), formally acting as NO-dioxygenase, yielding the harmless nitrate ion. X-ray crystal structures have shown that trHbN hosts a two-branched protein matrix tunnel system, proposed to control diatomic ligand migration to the heme, as the rate-limiting step in NO conversion to nitrate. Extended molecular dynamics simulations (0.1  $\mu$ s), employed here to characterize the factors controlling diatomic ligand diffusion through the apolar tunnel system, suggest that O<sub>2</sub> migration in deoxy-trHbN is restricted to a short branch of the tunnel, and that O<sub>2</sub> binding to the heme drives conformational and dynamical fluctuations promoting NO migration through the long tunnel branch. The simulation results suggest that trHbN has evolved a dual-path mechanism for migration of O<sub>2</sub> and NO to the heme, to achieve the most efficient NO detoxification. *Proteins* 2006;64:457–464.

© 2006 Wiley-Liss, Inc.

**Key words:** molecular dynamics; *M. tuberculosis*; ligand migration; nitric oxide

## INTRODUCTION

*Mycobacterium tuberculosis* is the causative agent of human tuberculosis,<sup>1</sup> a disease that infects about one-third of the human population, causing more than a million deaths per year. It has been reported that nitric oxide is produced in the macrophages during the initial growth infection stage, and that it may be involved in restricting the bacteria into latency.<sup>2</sup> The reaction of nitric oxide (NO) with the oxygenated form of “truncated hemoglobin” N (trHbN) has been proposed to be responsible for the resistance mechanism by which this microorganism can evade the toxic effects of NO, by acting as NO-dioxygenase to yield the harmless nitrate ion.<sup>3,4</sup>

Truncated hemoglobins (trHb) build a distinct group within the hemoglobin (Hb) superfamily that is widely distributed in bacteria, unicellular eukaryotes, and higher plants.<sup>5</sup> The tertiary structure of trHbs consists of a 2-on-2 helical sandwich that is a subset of the 3-on-3 sandwich of the classical globin fold.<sup>6</sup> The proximal HisF8 heme-linked residue is conserved in both Hb and trHb families, and a distal tyrosine at position B10 is found in almost all the trHb family members sequenced to date. Despite their small size compared to vertebrate globins, several trHbs host a protein matrix apolar tunnel system that connects the heme pocket with the protein surface.<sup>7–9</sup> In trHbN from *M. tuberculosis* the tunnel system is built by two perpendicular branches,<sup>8</sup> of about 8 and 20 Å length, respectively (Fig. 1), that have been proposed to control diatomic ligand diffusion to/from the heme<sup>10,11</sup> as the rate-limiting step in NO conversion to nitrate.<sup>12</sup>

Despite the biophysical and structural characterization of trHbN and the large number of studies on ligand migration to the heme in related proteins,<sup>13–17</sup> no detailed information is available on the molecular mechanisms underlying diffusion of both O<sub>2</sub> and NO in trHbN. Additionally, nothing is known on how *M. tuberculosis* trHbN regulates ligand access to the heme to achieve NO detoxification and survival of the mycobacterium under the nitro-

The first two authors contributed equally to this work.

Grant sponsor: Fundación Antorchas, Universidad de Buenos Aires; Grant number: X038; Grant sponsor: ANPCYT; Grant number: 06-08447; Grant sponsor: Spanish Ministerio de Investigación y Ciencia; Grant number: SAF2002-02482; Grant sponsor: NIH postdoctoral fellowship to M.M.; Grant number: 1-R01-AI052258 (2004–2007); Grant sponsor: CIMA (Milano, Italy) to M.B.; Grant sponsor: Fondazione CARIPLO (Milano, Italy) to M.B.; Grant sponsor: the Italian Ministry for University and Scientific Research FIRB Project “Biologia Strutturale”; Grant number: RBLA03B3KC, to M.B.

\*Correspondence to: Darío Estrin, University of Buenos Aires, Department of Chemistry, Ciudad Universitaria, Pab. 2, Buenos Aires, C1428EHA, Argentina or F. Javier Luque, University of Barcelona Av. Diagonal 643, 08028, Barcelona, Spain. E-mail: dario@qi.fcen.uba.ar or ffluque@ub.edu

Received 17 November 2005; Revised 3 February 2006; Accepted 15 February 2006

Published online 10 May 2006 in Wiley InterScience (www.interscience.wiley.com). DOI: 10.1002/prot.21004

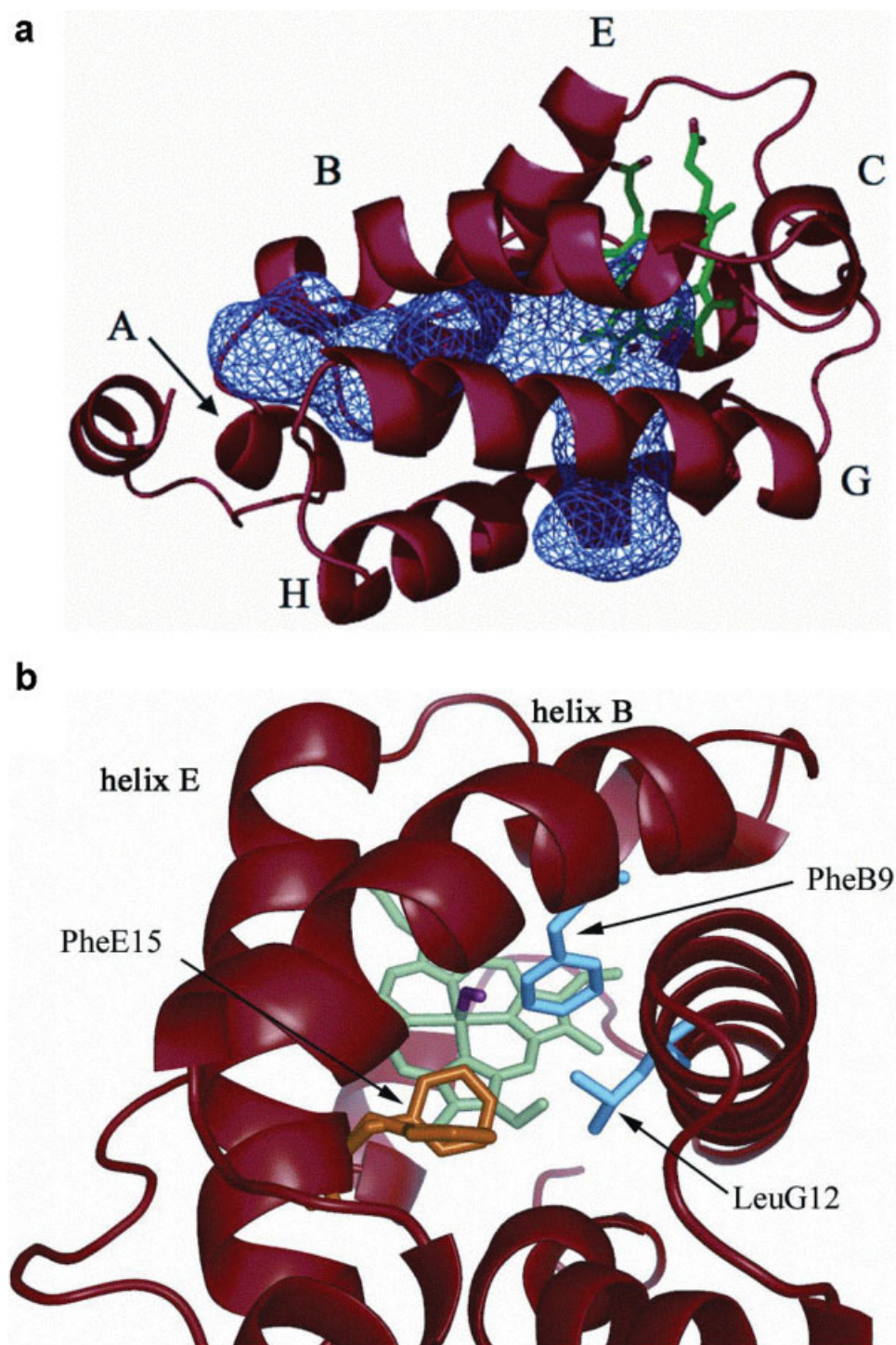


Fig. 1. (a) X-ray crystal structure of oxy-trHbN (PDB entry 1IDR) used in simulations, showing the labels of the helices, the location of the heme group (green) and the two branches of the tunnel system (blue mesh). The long branch ( $\sim 20$  Å long) is horizontal in the figure, and can be seen as roughly perpendicular to the heme distal face. The short branch ( $\sim 8$  Å long) lies roughly parallel to the heme plane (vertical in the figure), accessing the heme distal site pocket from the inner part of the heme crevice. Residues 1–15, building the N-terminal helix, are highlighted in purple. (b) Conformational change of PheE15 (orange) side chain along the  $C_{\alpha}$ – $C_{\beta}$  dihedral angle leading to *open* and *closed* states viewed along the tunnel long branch leading to the heme (green) in oxy-trHbN. The residues that define the bottleneck to ligand migration (PheB9, LeuG12; blue) in the *closed* state are also shown.

sative stress typical of latency conditions. Such mechanism issues are considered and explored in this work through extended 0.1- $\mu$ s molecular dynamics (MD) simulations of both oxy and deoxy forms of trHbN.

## MATERIALS AND METHODS

Molecular dynamics simulations were performed starting from the crystal structure of wild-type oxy-trHbN (PDB entry 1idr; monomer A at 1.9-Å resolution).<sup>8</sup> The enzyme was immersed in a preequilibrated octahedral box of TIP3P<sup>18</sup> water molecules. The standard protonation state at physiological pH was assigned to the ionizable residues. The final system contains the model protein, around 8600 water molecules and the added counterions, leading to a total of  $\sim 28,270$  atoms. Simulations were performed in the NPT (1 atm, 298 K) ensemble.<sup>19</sup> The system was simulated employing periodic boundary conditions and Ewald sums (grid spacing of 1 Å) for treating long range electrostatic interactions.<sup>20</sup> All simulations were performed with the parmm99 force field<sup>21</sup> using Amber8.<sup>22</sup> The initial system was minimized using a multistep protocol. First, the position of all hydrogens in the protein was refined by using 2000 cycles of energy minimization (500 cycles of steepest descent + 1500 cycles of conjugate gradient). Then, water molecules were refined using 10,000 cycles of energy minimization (2000 cycles of steepest descent + 8000 cycles of conjugate gradient). Finally, the position of all atoms in the system was energy minimized (2000 cycles of steepest descent + 8000 cycles of conjugate gradient). The equilibration process was performed by heating from 100 to 298 K in four 100-ps steps, and the final structure was used as the starting point for a 0.1- $\mu$ s MD simulation. To avoid a bias in the structure of the deoxy form of trHbN, it was built up by deleting the O<sub>2</sub> molecule from the X-ray crystallographic structure, and minimized and equilibrated following the same protocol mentioned above. The oxygenated and deoxygenated heme model system charges were determined by using RESP charges<sup>23</sup> and HF/6-31G(d) wave functions, according to the Amber standard protocol.

To study in detail the properties of the tunnel cavity system in trHb N from *M. tuberculosis*, we have calculated the diffusion free energy profiles for a diatomic neutral ligand along the tunnels for the oxy and deoxy proteins. The free energy profiles were constructed by performing constant velocity multiple steering molecular dynamics (MSMD) simulations, and using the Jarzynski's inequality,<sup>24</sup> which relates equilibrium free energy values with the irreversible work performed over the system that proceeds along a reaction coordinate from reactants to products. In the present study, the reaction coordinate  $\lambda$  was chosen as the iron–ligand distance. Calculations were performed using a force constant of 200 kcal  $\cdot$  mol<sup>-1</sup> Å<sup>-1</sup> and pulling velocities of 0.05 and 0.1 Å/ps, which yielded similar free energy profiles. The statistical error was calculated as the standard deviation between these two estimates. To reconstruct the free energy profile of ligand migration along the tunnels, a set of MSMD runs were performed starting from equilibrated MD structures with  $\lambda$  ( $t = 0$ ) corresponding

with the ligand in (1) the distal pocket, (2) the crystallographic Xe-binding sites, and (3) the ligand outside the tunnels. Ten MSMD simulations were performed in each direction (forward/exit and backward/entry) for each of the two pulling velocities. In cases in which two overlapping profiles were obtained (from entry and exit sets), we confirmed that both of them matched.

The role of PheE15 as gate residue along the long branch of the tunnel was investigated by computing the free energy profile using umbrella-sampling techniques<sup>20</sup> for the oxy and deoxy states of the proteins, using the PheE15 C $_{\alpha}$ –C $_{\beta}$  dihedral angle as distinguished coordinate and a set of 12 windows of 1 ns each. Two independent sets of 12 windows each were employed to estimate the statistical error.

Finally, the set of structures collected along the 0.1- $\mu$ s MD simulations were used to explore the dynamical behavior of the protein by determining the essential dynamics through principal component analysis,<sup>25</sup> conducted considering the backbone C $_{\alpha}$  atoms. Indeed, residues 1–15, which form the short N-terminal isolated helix (Fig. 1), were also excluded from the analysis because high flexibility in this region might mask the essential movements in the trHbN fold.

## RESULTS AND DISCUSSION

To address the question of how NO can access the heme in oxy-trHbN, we analyzed a 0.1- $\mu$ s trajectory of oxy-trHbN. The analysis revealed that only the long branch of the tunnel remains open for a significant fraction of time to allow diffusion of NO, and that opening of this path is controlled by residue PheE15, whose side chain mainly populates two conformations [characterized by average C $_{\alpha}$ –C $_{\beta}$  torsional angles of about +40 and –50 degrees; Fig. 2(a)]. In the PheE15 *closed* state the side-chain phenyl ring protrudes into the tunnel long branch, preventing the access of incoming ligands to the heme distal cavity through this path. On the contrary, in the *open* state, PheE15 is roughly parallel to the tunnel long branch axis, enabling the transit of diatomic ligands, the narrowest tunnel width being  $\sim 3.4$  Å.

The free energy profiles for ligand migration, obtained through steered MD simulations, indicated that in the *open* state NO diffusion is almost free of barriers, and access to the heme cavity is favored by 3–4 kcal/mol [Fig. 2(b)]. On the contrary, in the *closed* state the steric hindrance of PheE15 phenyl ring undermines ligand access, leading to a steady increase in the free energy profile [Fig. 2(b)]. Interestingly, the free energy minimum found at about 11 Å from the heme matches one of the Xe binding sites observed experimentally in *M. tuberculosis* trHbN.<sup>9</sup> Steered MD simulations also revealed that in oxygenated trHbN migration of NO through the tunnel short branch is not favored, related to a progressive rise in the free energy [Fig. 2(c)]. Taken together, the above results suggest that NO access to the heme distal cavity should preferentially occur through the long tunnel branch in oxy-trHbN.

Strikingly, the ligand migration pathway described above is drastically different in deoxy-trHbN. The analysis of the



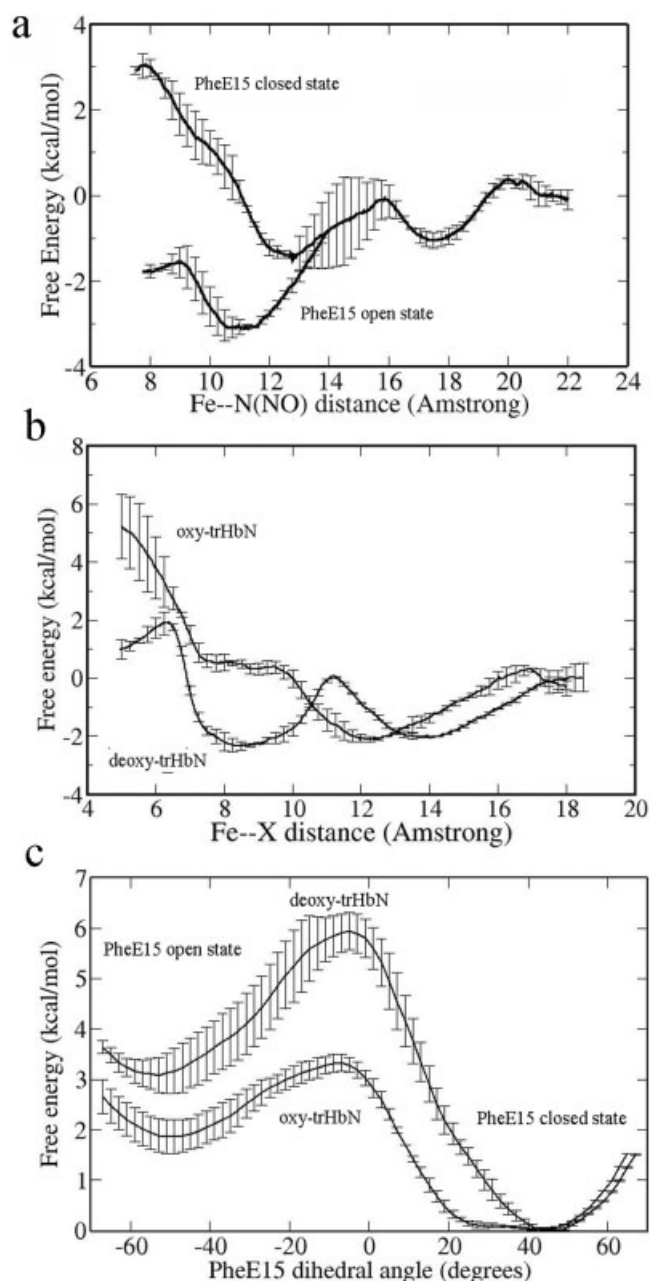


Fig. 2. (a) Free energy profile for NO migration along the long tunnel branch in both *open* and *closed* states of oxy-trHbN; the distance from the Fe atom to the nitrogen in NO is used as the driven coordinate. (b) Free energy profile for diatomic ligand (NO; O<sub>2</sub>) migration along the short tunnel branch for oxy-trHbN (NO) and deoxy-trHbN (O<sub>2</sub>); the distance from the Fe atom to either nitrogen (NO) or oxygen (O<sub>2</sub>) atoms is used as the driven coordinate. (c) Potential of mean force for the conformational change in PheE15 C<sub>α</sub>–C<sub>β</sub> dihedral angle leading to conversion between open and closed states in deoxy- and oxy-trHbN. The statistical error bars were computed as stated in Material and Methods.

0.1-μs MD trajectory for deoxy-trHbN showed that the long branch of the tunnel remains closed during the whole simulation time. In fact, the PheE15 torsional free energy profile, obtained using umbrella sampling calculations, reveals that in deoxy-trHbN the conformational transition between *open* and *closed* states of the tunnel gating

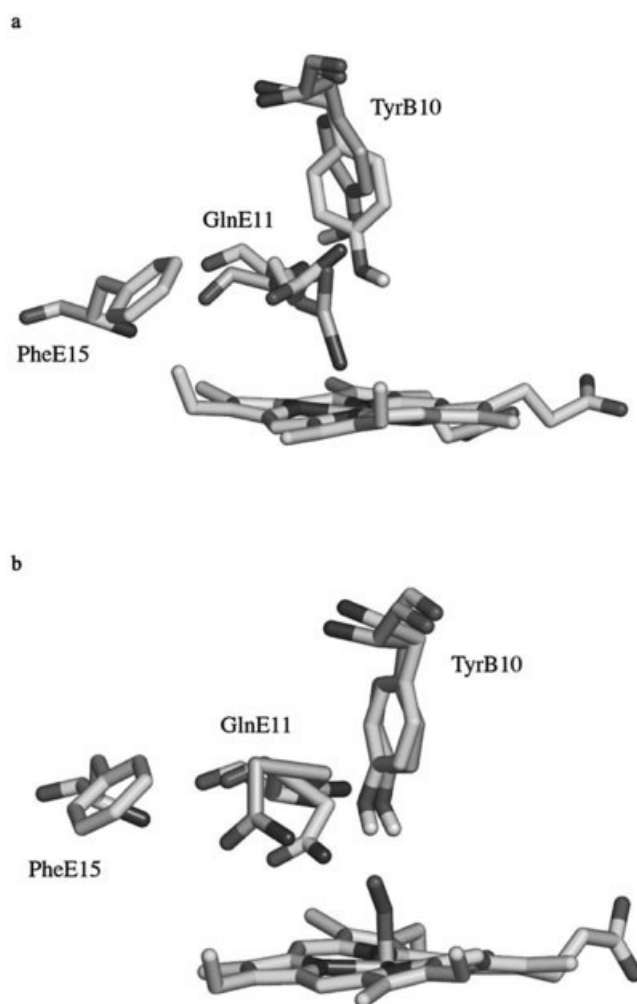


Fig. 3. Interactions between TyrB10 and GlnE11 in deoxy-trHbN and oxy-trHbN. (a) In deoxy-trHbN, the side chain of GlnE11 adopts an *all-trans* conformation (average torsions around C<sub>α</sub>–C<sub>β</sub>, C<sub>β</sub>–C<sub>γ</sub>, and C<sub>γ</sub>–C<sub>δ</sub> dihedrals of 40.2, 167.1, and 93.7 degrees), although the relative orientation of the amide group of GlnE11 and hydroxyl group of TyrB10 fluctuate along the trajectory. (b) In oxy-trHbN the side chain of GlnE11 populates two *staggered* conformation characterized by torsional angles around C<sub>α</sub>–C<sub>β</sub>, C<sub>β</sub>–C<sub>γ</sub>, and C<sub>γ</sub>–C<sub>δ</sub> bonds of (+45.0, –74.8, –99.3 degrees) and (–50.2, +67.2, +48.5 degrees), respectively. Transition of the former conformation to the latter one makes GlnE11 to approach PheE15 by ~1.5 Å.

residue PheE15 must overcome a free energy barrier higher than 6 kcal/mol (compared with the 3 kcal/mol barrier of oxy-trHbN; see Fig. 3). Moreover, the *open* state (less stable by ~2 kcal/mol relative to the *closed* state in oxy-trHbN) is further destabilized by 1.5 kcal/mol in deoxy-trHbN. In contrast, ligand migration through the short branch of the tunnel is now allowed, with a small free energy barrier [~2 kcal/mol; Fig. 2(c)] before reaching a flat minimum, which corresponds to a cavity formed by residues PheG5, AlaG9, and IleH11. In fact, this cavity is one of the Xe binding pockets observed by X-ray crystallography in the short tunnel branch.<sup>9</sup> Access to the Fe atom from this cavity requires overcoming a free energy barrier of ~4 kcal/mol [Fig. 2(c)], reflecting a narrow passage through the heme and ValG8.

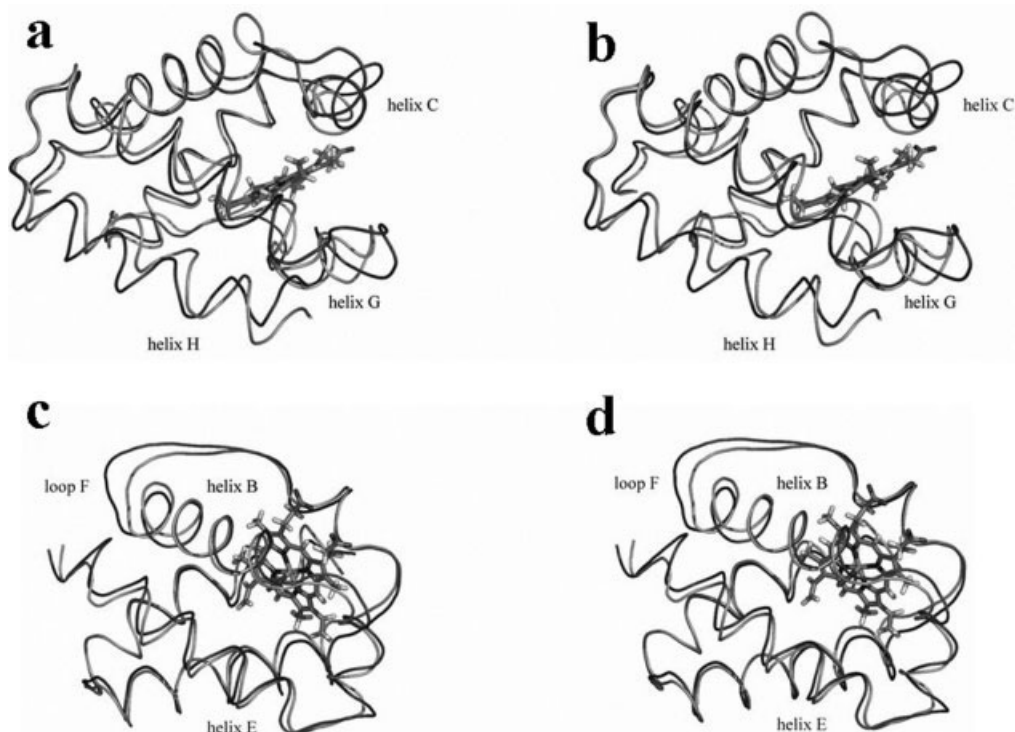


Fig. 4. Stereoview of the essential dynamics results of two different snapshots for deoxy-trHbN (a and b) and for oxy-trHbN (c and d). The largest motion leading to dynamical fluctuations in the protein backbone and the structural elements mainly involved in those fluctuations are shown.

The preceding results suggest that *M. tuberculosis* trHbN has evolved a molecular mechanism for ligand diffusion, whereby the coordination state of the heme group modulates the main path for ligand entry. Thus, access of an  $O_2$  molecule to the heme through the tunnel short branch, and its coordination to the heme-Fe atom, would facilitate migration of the second ligand (NO; alternatively another  $O_2$  molecule) through the tunnel long branch.

Such first set of conclusions raises the question of how does  $O_2$  binding to the heme regulate the ligand access pathway. Our simulation results indicate that such regulation may be achieved through alteration of the heme distal site hydrogen-bonded network, a structural feature previously recognized to play a key role in trHbN heme/ligand stabilization.<sup>7,10</sup> In the deoxy-trHbN simulation, the side chain of GlnE11 adopts an extended *all-trans* conformation, allowing the terminal amido group to be hydrogen-bonded to the hydroxyl group of TyrB10. In addition, the simulation shows a dynamical fluctuation between (TyrB10)O—H  $\cdots$  O=C(GlnE11) and (TyrB10)O  $\cdots$  H—N(GlnE11) hydrogen bonds, such that TyrB10 hydroxyl group acts both as hydrogen-bond donor and acceptor in the 0.1- $\mu$ s time frame (Fig. 4). In contrast, in oxy-trHbN the heme-Fe coordinated  $O_2$  restricts the conformational freedom of TyrB10 through a hydrogen bond, thus allowing the phenolic hydroxyl group to act exclusively as hydrogen-bond acceptor for the amide- $NH_2$  group of GlnE11. Under these conditions GlnE11 side chain is forced to fluctuate between two *staggered* conformations (Fig. 4), and the distance between the side chains of

GlnE11 and PheE15 is shortened by  $\sim 1.5$  Å, due to different residue packing. Thus, GlnE11 might be viewed as an internal “switch” that would regulate the *open/closed* state of the PheE15 gate, within the tunnel long branch through a conformational compression mechanism (Fig. 4).

The changes in the heme distal site local structure, however, are also linked to alteration of the protein backbone motions. Thus, essential dynamics analysis shows that in deoxy-trHbN the major motions affect helices C, G, H, and the F extended region. In contrast, when opening/closing events occur in the tunnel long branch, the major motion in oxy-trHbN involves the relative displacement of helices B and E (see Fig. 4). These findings therefore suggest that binding of  $O_2$  to the heme group triggers a large-scale dynamical change that alters the natural fluctuations in the protein backbone, in agreement with the available experimental evidence indicating that ligand binding modulates trHbN structural plasticity.<sup>26</sup> In view of the specific location of GlnE11 within the protein structure, it can be speculated that the conformational “switch” described above for this residue may also play a role in facilitating the relative motion of helices B and E and the opening of the PheE15 gate.

The analysis of oxy-trHbN MD trajectory additionally revealed that the relative displacement of helices B and E is also regulated by the formation of a salt bridge between Arg10 (in the N-terminal region) and Glu70 (in the EF interhelical region) (Fig. 5), which promotes folding of the short A helix onto the EF hinge. As a result, helix E cannot

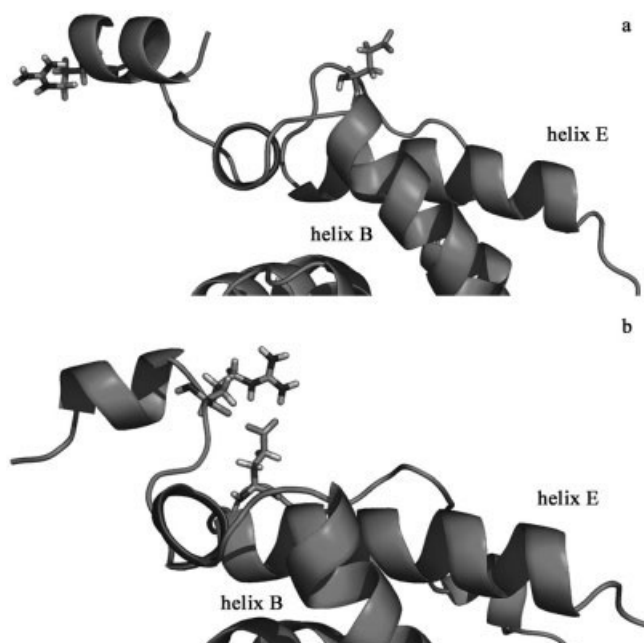


Fig. 5. The Arg10–Glu70 salt bridge interaction in trHbN. (a) In the absence of the salt bridge the dynamical fluctuations of the protein backbone facilitates the relative displacement of helices B and E, which should facilitate opening of the PheE15 gate in the tunnel long branch. (b) Formation of the salt bridge inhibits ligand migration through the tunnel long branch by increasing the friction between helices B and E.

be displaced relative to helix B, and the enhanced friction inhibits opening of the long tunnel branch. These results are consistent with the experimentally observed dependence of the kinetics of ligand diffusion in trHbN on the viscosity of the aqueous environment.<sup>10,11</sup>

On the basis of the preceding results, a dual-path ligand-induced regulation mechanism is proposed to be operative in *M. tuberculosis* trHbN. The key feature in such mechanism is the change of contacts formed by TyrB10 and GlnE11. Thus, O<sub>2</sub> binding to the heme would promote a *local* conformational change in the TyrB10–GlnE11 pair, in turn inducing compression on PheE15, facilitating the relative displacement of helices B and E and altering the *global* dynamical fluctuations of the protein. The alteration of the essential dynamics, in conjunction with rearrangements in the side chains that surround PheE15, would promote opening of the tunnel long branch, enhancing capture of NO from the aqueous phase. This mechanism partly relies on the very high oxygen affinity of the protein (O<sub>2</sub> binding affinity to ferrous trHbN of  $8.0 \times 10^{-9}$  M),<sup>7</sup> which guarantees that it is mainly loaded with O<sub>2</sub>. The mechanism also benefits from the high hydrophobic character of the ligand diffusion tunnel, which can act as a potential reservoir to concentrate nonpolar diatomic ligands (possibly in the identified Xe sites), at the same time limiting the rate at which water may occupy the heme pocket, when vacated by the dissociated ligand. All these factors would contribute to enhance the efficiency of NO detoxification. The mechanism also

provides a basis to rationalize why NO conversion to nitrate by oxy-trHbN occurs at a rate faster than O<sub>2</sub> binding to the deoxy protein (bimolecular rate constants of 745 and 25  $\mu\text{M}^{-1} \text{s}^{-1}$ , respectively),<sup>3,7</sup> an explanation that cannot be extracted from the X-ray structures and from the kinetic data alone.

Our results are also consistent with recent studies of the modulation of the kinetics of CO recombination in trHbN, which suggest the existence of different ligand-dependent conformations with different kinetic behaviours.<sup>11</sup> Thus, these studies showed that the kinetic patterns observed for CO recombination to trHbN, which are atypical when compared with many other hemoglobins and myoglobins, exhibit up to three kinetic phases. It was shown that the time scale of the slowest phase is within experimental error consistent with the association of the binding of CO to deoxy trHbN, and that its amplitude increases with decreasing viscosity or increasing temperature. These experimental observations were interpreted by assigning the slowest phase to a CO rebinding process under conditions where the heme environment has fully relaxed to a conformation or distribution of conformations associated with the deoxy form of trHbN. In fact, it was concluded that a different range of conformations is accessible for the protein depending on the coordination state of the heme group, in agreement with our simulation results indicating that the dynamical fluctuations of trHbN are drastically altered upon binding of O<sub>2</sub> to the heme. It should also be noticed that the ligand-induced trHbN structural plasticity has also been highlighted by comparison of the UV Raman spectra of the w.t. protein with the TyrB10 → Phe mutant upon NO binding.<sup>26</sup> These spectroscopic measurements clearly indicate that NO binding to the heme distal site triggers a large-scale conformational change that propagates through the pre-F helix to the E and B helices, in keeping with the large changes in the natural dynamics of the protein observed in the MD simulations of both deoxy- and oxy-forms of trHbN.

There are also relevant differences in the CO recombination process for w.t. trHbN and its TyrB10 → Phe mutant, which have been attributed to differences in the relaxation of the aromatic side chain at B10.<sup>11</sup> Whereas for the w.t. protein there is a phase corresponding to a viscosity-dependent relaxation initiated upon ligand dissociation, a single, faster, CO recombination process is experimentally observed for the mutant. This finding suggests a critical role played by TyrB10, which can be interpreted in terms of its hydrogen bond interaction with GlnE11. Thus, even though our results indicate that hydrogen bonding between these two residues is present in both deoxy- and oxy-states of trHbN, O<sub>2</sub> binding to the heme promotes a local conformational rearrangement of the TyrB10–GlnE11 pair, which ultimately modulates the conformational space accessible to the protein leading to the opening of the long branch tunnel. Replacement of TyrB10 by Phe removes such hydrogen bond, preventing the onset of the ligand-induced conformational switch mechanism; this



would also explain the different kinetic behavior seen in the TyrB10 → Phe mutant.

## CONCLUSIONS

The present results suggest that a novel dual-path ligand-induced regulation mechanism is operative in *M. tuberculosis* trHbN, whereby the protein dynamics and the protein matrix tunnel system have evolved to allow the access of O<sub>2</sub> and NO ligands to the heme through distinct migration paths. The key feature in such mechanism is the change of contacts formed by TyrB10 and GlnE11, where GlnE11 acts as a switch regulating the ligand access pathway by altering the essential movements of the protein backbone. Thus, O<sub>2</sub> binding to the heme should induce compression of PheE15 by the side chain of GlnE11, and promote the relative displacement of helices B and E. These events, combined with local rearrangements in the side chains that surround PheE15, should open the tunnel long branch, facilitating capture of NO from the aqueous phase.

The detailed microscopic information obtained in these simulation studies suggests mutations that would significantly effect O<sub>2</sub>/NO multiligand chemistry. Specifically, mutations of the gate amino acid PheE15 to Ala or Trp should promote full opening or permanent closing of the gate, respectively. Mutation of TyrB10 and GlnE11 should also greatly affect the conformational changes that lead to the opening of the tunnel long branch upon O<sub>2</sub> binding. Finally, to complete a full cycle, the nitrate anion produced should be removed from the heme cavity, and the Fe(III) protein should be reduced back to Fe(II). How these processes are accomplished is still unknown, although nitrate efflux to the solvent is expected to be fast, and probably limited by the heme–nitrate bond breaking. A suitable reductase system is expected to control the heme–Fe atom redox state in vivo, considering that steady conversion of NO to nitrate is an established protection mechanism in *M. tuberculosis*.<sup>2,3</sup>

As a final consideration, we note that other heme proteins have been proposed to perform multiligand chemistry. Among these, oxy-hemoglobin, oxy-myoglobin, and the recently discovered neuroglobin and cytoglobin.<sup>27–29</sup> Untangling the structural determinants of the interplay between ligand binding, protein dynamics and ligand migration will be essential to shed light on the emerging field of multiligand chemistry performed by heme proteins.

## ACKNOWLEDGMENTS

Calculations were performed in the MareNostrum supercomputer at the Barcelona Supercomputing Center.

## REFERENCES

- Bloom BR. Tuberculosis: pathogenesis, protection and control. Washington, DC: ASM Press; 1994.
- MacMicking JD, North RJ, LaCourse R, Mudgett JS, Shah SK, Nathan CF. Identification of nitric oxide synthase as a protective locus against tuberculosis. *Proc Natl Acad Sci USA* 1997;94:5243–5248.
- Ouellet H, Ouellet Y, Richard C, Labarre M, Wittenberg B, Wittenberg J, Guertin M. Truncated hemoglobin HbN protects *Mycobacterium bovis* from nitric oxide. *Proc Natl Acad Sci USA* 2002;99:5902–5907.
- Couture M, Yeh SR, Wittenberg BA, Wittenberg JB, Ouellet Y, Rousseau DL, Guertin M. A cooperative oxygen-binding hemoglobin from *Mycobacterium tuberculosis*. *Proc Natl Acad Sci USA* 1999;96:11223–11228.
- Moens L, et al. Globins in nonvertebrate species: dispersal by horizontal gene transfer and evolution of the structure–function relationships. *Mol Biol Evol* 1996;13:324–333.
- Pesce A, Couture M, Dewilde S, Guertin M, Yamauchi K, Ascenzi P, Moens L, Bolognesi M. A novel two-over-two alpha-helical sandwich fold is characteristic of the truncated hemoglobin family. *EMBO J* 2000;19:2424–2434.
- Milani M, Pesce A, Nardini M, Ouellet H, Ouellet Y, Dewilde S, Bocedi A, Ascenzi P, Guertin M, Moens L, Friedman JM, Wittenberg JB, Bolognesi M. Structural bases for heme binding and diatomic ligand recognition in truncated hemoglobins. *J Inorg Biochem* 2005;99:97–109.
- Milani M, Pesce A, Ouellet Y, Ascenzi P, Guertin M, Bolognesi M. *Mycobacterium tuberculosis* hemoglobin N displays a protein tunnel suited for O<sub>2</sub> diffusion to the heme. *EMBO J* 2001;20:3902–3909.
- Milani M, Pesce A, Ouellet Y, Dewilde S, Friedman JM, Ascenzi P, Guertin M, Bolognesi M. Heme–ligand tunneling in group I truncated hemoglobins. *J Biol Chem* 2004;279:21520–21525.
- Samuni U, Dantsker D, Ray A, Wittenberg JB, Wittenberg BA, Dewilde S, Moens L, Ouellet Y, Guertin M, Friedman JM. Kinetic modulation in carbonmonoxy derivatives of truncated hemoglobins: the role of distal heme pocket residues and extended apolar tunnel. *J Biol Chem* 2003;278:27241–27250.
- Dantsker D, Samuni U, Ouellet Y, Wittenberg BA, Wittenberg JB, Milani M, Bolognesi M, Guertin M, Friedman JM. Viscosity-dependent relaxation significantly modulates the kinetics of CO recombination in the truncated hemoglobin TrHbN from *Mycobacterium tuberculosis*. *J Biol Chem* 2004;279:38844–38853.
- Crespo A, Martí MA, Kalko SG, Morreale A, Orozco M, Gelpi JL, Luque FJ, Estrin DA. Theoretical study of the truncated hemoglobin HbN: exploring the molecular basis of the NO detoxification mechanism. *J Am Chem Soc* 2005;127:4433–4444.
- Schotte F, Lim M, Jackson TA, Smirnov AV, Soman J, Olson JS, Phillips GN Jr, Wulff M, Anfinsen PA. Watching a protein as it function with 150 ps time resolved X-ray crystallography. *Science* 2003;300:1944–1947.
- Chu K, Vojtechovsky J, McMahon BH, Sweet RM, Berendzen J, Schlichting I. Structure of a ligand binding intermediate in wild type carbonmonoxy myoglobin. *Nature* 2000;403:921–923.
- Case DA, Karplus M. Dynamics of ligand binding to heme proteins. *J Mol Biol* 1979;132:343–368.
- Bossa C, Anselmi M, Roccatano D, Amadei A, Vallone B, Brunori M, Di Nola A. Extended molecular dynamics simulation of the carbon monoxide migration in sperm whale myoglobin. *Biophys J* 2004;86:3855–3862.
- Nutt DR, Meuwly M. CO migration in native and mutant myoglobin: atomistic simulations for the understanding of protein function. *Proc Natl Acad Sci USA* 2004;101:5998–6002.
- Jorgensen WL, Chandrasekhar J, Madura JD, Impey RW, Klein ML. Comparison of simple potential functions for simulating liquid water. *J Chem Phys* 1983;79:926–935.
- Berendsen HJC, Postma JPM, van Gunsteren WF, Di Nola A, Haak JR. Molecular dynamics with coupling to an external bath. *J Chem Phys* 1984;81:3684–3690.
- Leach AR. Molecular modelling. 2nd ed. Englewood Cliffs, NJ: Prentice Hall; 2001.
- Wang J, Cieplak P, Kollman PA. How well does a restrained electrostatic potential (RESP) model perform in calculating conformational energies of organic and biological molecules? *J Comput Chem* 2000;21:1049–1074.
- Pearlman DA, Case DA, Caldwell JW, Ross WR, Cheatham TE III, DeBolt S, Ferguson D, Seibel G, Kollman P. AMBER, a computer program for applying molecular mechanics, normal mode analysis, molecular dynamics and free energy calculations to elucidate the structures and energies of molecules. *Comp Phys Commun* 1995;91:1–41.
- Bayly CI, Cieplak P, Cornell W, Kollman PA. A well behaved electrostatic potential based method using charge restraints for

- deriving atomic charges: the RESP model *J Phys Chem* 1993;97:10269–10280.
24. Jarzynski C. Non equilibrium equality for free energy differences. *Phys Rev Lett* 1997;78:2690–2693.
  25. Amadei A, Linssen ABM, Berendsen HJC. Essential dynamics of proteins. *Proteins* 1993;17:412–415.
  26. Mukai M, Ouellet Y, Guertin M, Yeh S-R. NO binding induced conformational changes in a truncated hemoglobin from *Mycobacterium tuberculosis*. *Biochemistry* 2004;43:2764–2770.
  27. Ascenzi P, Salvati L, Brunori M. Does myoglobin protect *Trypanosoma cruzi* from the antiparasitic effects of nitric oxide? *FEBS Lett* 2001;501:103–105.
  28. Eich RF, Li T, Lemon DD, Doherty DH, Curry SR, Aitken JF, Mathews AJ, Johnson KA, Smith RD, Phillips GN Jr, Olson JS. Mechanism of NO-induced oxidation of myoglobin and hemoglobin. *Biochemistry* 1996;35:6976–6983.
  29. Brunori M, Giuffrè A, Nienhaus K, Ulrich Nienhaus G, Scandurra FM, Vallone B. Neuroglobin, nitric oxide, and oxygen: functional pathways and conformational changes. *Proc Natl Acad Sci USA* 2005;102:8483–8488.